Scientia Iranica A (2021) 28(2), 618–628

SCIENTIA IRANICA

Sharif University of Technology
Scientia Iranica
Transactions A: Civil Engineering
http://scientiairanica.sharif.edu

Damping estimation of a double-layer grid by output-only modal identification

S.R. Nabavian[a], M.R. Davoodi[a,*], B. Navayi Neya[a], and S.A. Mostafavian[b]

a. *Faculty of Civil Engineering, Babol Noshirvani University of Technology, Babol, P.O. Box 484, Iran.*
b. *Department of Civil Engineering, Payame Noor University (PNU), Tehran, P.O. Box 19395-3697, Iran.*

Received 1 October 2018; received in revised form 21 October 2019; accepted 21 December 2019

KEYWORDS
Modal damping ratio;
Modal testing;
Output-only methods;
Double-layer grid;
Ball-joint system.

Abstract. Modal parameters of large civil engineering structures such as Modal Damping Ratios (MDRs) are determined mainly through output-only modal identification. In this paper, MDRs of a double-layer grid were obtained using output-only modal identification. For this purpose, a double-layer grid constructed of a ball-joint system was tested. Through some random tapping on the structure, the acceleration response in multiple locations was measured. The acquired data were processed using output-only modal identification to arrive at MDRs. The MDRs corresponding to the first eight modes of the grid were extracted by five output-only modal identification techniques, namely Enhanced Frequency Domain Decomposition (EFDD), Curve-fit Frequency Domain Decomposition (CFDD), and three different methods of data-driven stochastic subspace identification. To determine the appropriate model order used in SSI methods, sensitivity analysis was carried out and the resulting number of orders was 200. The proper frequency resolution of 1600 was determined to estimate the MDRs of the grid by EFDD and CFDD. The results showed that the MDRs of the grid obtained from different methods were in good agreement with each other. The grid has very low MDRs because the MDRs of the modes measured using different methods varied from 0.06% to 0.11%.

1. Introduction

Double-layer grids constitute an important family of space structures. A double-layer grid consists of two parallel layers of elements that are connected together with web elements. High stiffness to weight ratio, ease and speed of handling, and favorable architectural appearance are the reasons why these types of structures are widely employed to cover large spans without any intermediate support. In double-layer grids, there are many joints with complexities such as the presence of different materials, the bolt and pre-stress force, and the gaps between contact components [1]. Although double-layer grids are becoming widespread today, their dynamic behavior has not been sufficiently studied.

One of the important factors influencing the dynamic behavior of a structure is its damping. The significance of damping lies in its maximum dynamic response to a certain excitation and in determining the number of vibration cycles required to reduce the dynamic amplitude. Owing to the complexity of the damping mechanisms and several sources used for damping in a structure, it is often not possible to give a proper analytical estimate; hence, experimental tests are required [2,3]. The most common method of experimental tests for structural vibration is modal

*. *Corresponding author. Tel./Fax: +981132331707*
E-mail addresses: r.nabavian.h@gmail.com (S.R. Nabavian); davoodi@nit.ac.ir (M.R. Davoodi); navayi@nit.ac.ir (B. Navayi Neya); amin.mostafavian@gmail.com (S.A. Mostafavian)

doi: 10.24200/sci.2019.51919.2424

testing in which the effect of all different damping mechanisms is incorporated using an Modal Damping Ratio (MDR) for each vibration mode [4].

Experimental determination of the MDR as one of the structural parameters can be done through:

1. Input-output modal identification;
2. Output-only modal identification.

The MDRs in the input-output identification methods are determined based on input excitation and output response of a structure. However, the MDRs in the output-only modal identification are determined only by output response measurements. Given the input-output modal identification must be done by controlling the input, it is often used in the lab environment. However, the modal identification of large structures such as double-layer grids must be determined by the output-only modal identification method.

There are numerous references that perform damping estimation through output-only modal identification method. Bajric et al. [5] determined the damping of a two-degree-of-freedom system using different time-domain output-only modal identification methods. The results showed that there were notable differences in accuracy of different techniques. For example, one can make a reference to damping estimation in civil structures including Qingzhou cable suspension bridge in China [6] and Tennessee steel arc bridge in America [7]. Rainieri et al. [8] determined damping of the Tower of the Nation, Naples using output-only methods of data-driven stochastic system identification (SSI-DD), covariance-driven stochastic subspace identification (SSI-COV), and Enhanced Frequency Domain Decomposition (EFDD). Their results revealed an insignificant difference in MDRs identified using various methods. Bajric et al. [9] studied the sensitivity of damping estimates of closely spaced modes for two output-only methods of Eigensystem Realization Algorithm (ERA) and Frequency Domain Decomposition (FDD). They also investigated the reliability and accuracy of damping estimation using the two methods and concluded that the ERA was a more robust technique for estimating damping than the FDD. Gomaa et al. [10] obtained the MDRs for a two-story steel frame using EFDD and SSI methods. Their results showed that the MDR estimated by the EFDD was approximately twice the estimated value of the SSI. Bajric et al. [11] determined the MDR for an offshore wind turbine tower by the ERA, EFDD, and SSI-Cov methods. The results of their study revealed that the SSI-Cov method was more efficient in estimating damping than the two other methods. They also investigated the effects of noise in signal, measurement time, vibration amplitudes, and stationarity of the response on damping estimation. Kudu et al. [12] determined the MDRs of a three-story steel building using EFDD and SSI methods. Their results showed that although the change in natural frequencies was very insignificant, the MDRs varied considerably. Further examples of the quality of damping estimates through output-only methods can be found in [13,14]. Typically, modal damping estimates through output-only methods show greater dispersion than the estimates of the mode shape and natural frequency. The conducted research shows that there is no agreement on the accuracy and dispersion of damping estimates identified by different output-only methods. In some references such as [15,16], damping estimates with the output-only methods are often considered undesirable and inaccurate. Some other references including [17] revealed that damping estimates using the output-only method had high reliability and acceptable accuracy.

This paper focuses on the damping estimates of a double-layer grid constructed of the ball-joint system through output-only modal identification and determines whether the MDRs identified using different methods show significant dispersion or not. A comparison of five existing output-only techniques was made in providing damping estimates.

2. Double-layer grid

Regarding the laboratory constraints and considerations for real structures, a double-layer grid with a two-way on two-way configuration and the ball-joint system was constructed. The general dimensions of the grid in plan are equal to 565.6 cm × 424.2 cm and its height (distance between the top and bottom layers) is 100.0 cm. As shown in Figure 1, the bottom layer of the grid includes three spans of 141.4 cm in an extension and four spans of 141.4 cm perpendicular to it. The grid consists of 96 steel pipes (with an outer diameter of 7.64 cm and a thickness of 0.35 cm) and 32 balls. All components (members and balls) used to construct the grid are identical and the same as those used in practice. The total weight of the structure is approximately 8550 N [18].

To minimize the effects of supporting conditions on the modal parameters, the grid was tested in a free boundary condition. The grid was suspended by four springs from four nodes with the least average modal displacement.

3. Data acquisition

The equipment used to perform the modal testing includes a 4-channel B & K PULSE 3560 C spectral analyzer and 3 DJB (A/120/V) accelerometers.

In order to conduct output-only modal testing, the acceleration responses of 3 accelerometers were simultaneously measured and required in the identifi-

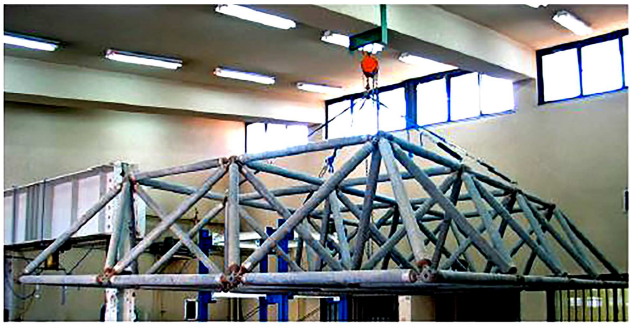

(a)

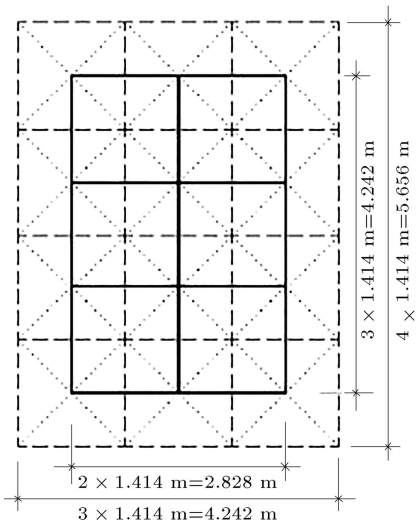

(b)

Figure 1. (a) general view and (b) plan of the double-layer grid [18].

cation process. The accelerometers should be installed in a node with the maximum average acceleration response. A corner ball of the bottom layer of the grid is characterized by the above property. By applying some random tapping to the grid, the resulting response was measured through three attached accelerometers in all of the three horizontal X, horizontal Y, and vertical Z directions. The tapping was applied accidently to different nodes in different directions. Given that determining the mode shapes of the grid was not the case, measuring the response of one node was sufficient. According to Eq. (1), the maximum measurement duration should fulfill the requirement such that [19]:

$$T > 10/(f_{\min} \times \xi), \tag{1}$$

where T is the response measurement duration, ξ is the MDR, and $f_{\min}$ is the lowest natural frequency of the structure. The use of information extracted from initial tests and Eq. (1) resulted in a record length of 840 s. The RMS levels of the acceleration responses ranged from 26 to 68 mm/s^2 with a median of 42 mm/s^2. The maximum peak values for the

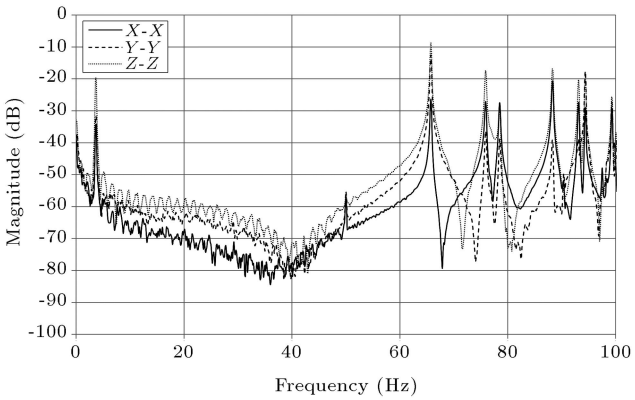

Figure 2. Power Spectral Density (PSD) function of acceleration responses in X, Y, and Z directions.

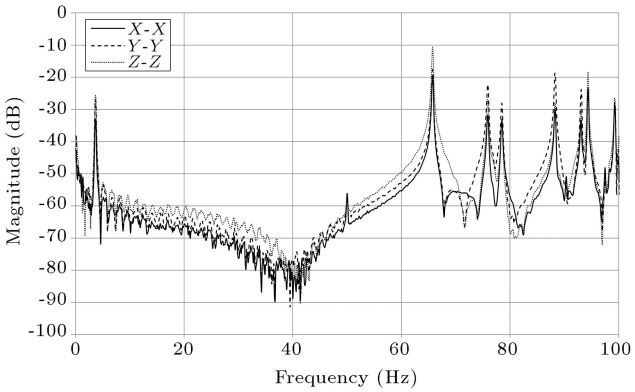

Figure 3. Cross Spectral Density (CSD) function of acceleration responses.

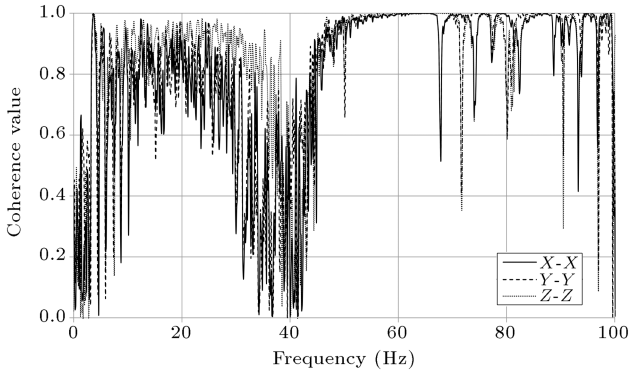

Figure 4. Coherence function of acceleration responses.

acceleration responses ranged from 0.6 to 1.5 m/s^2. The response sampling time step is 0.00195 s. The acceleration responses were measured at a rate of 512 Hz, resulting in the Nyquist frequency of 216 Hz, which is higher than the largest natural frequency of interest, that is, 100 Hz.

Figures 2 and 3 show the Power Spectral Density (PSD) and Cross Spectral Density (CSD) of responses. The coherence function of responses is given in Figure 4. In a well-made measurement, the coherence is unity around resonances as given clearly in Figure 4.

4. Data processing

The acquired responses from the output-only modal testing were processed via the time domain SSI-DD and frequency domain EFDD and CFDD methods for modal parameter extraction. All estimations were carried out using ARTeMIS Modal 4.0 software [20]. There are three various SSI algorithms in this software: Unweighted Principal Component (SSI-UPC), Principal Component (SSI-PC), and Canonical Variate Analysis (SSI-CVA), all of which have been applied to the estimation of modal parameters. The only significant difference between different SSI algorithms is the choice of weight matrices. Common SSI input matrix is pre- and post-multiplied by the aforementioned weight matrices to determine system matrices, as used for extraction of modal parameters. For a detailed description of the methods, readers are referred to [21,22]. The following is a brief description of the methods used.

SSI: SSI is a parametric time-domain method based on a state-space description of the dynamic problem. The SSI method was proposed by van Overschee and DeMoor. Peeters and De Roeck [23] used SSI to identify the modal parameters of engineering structures. Brincker and Andersen [24] formulated the mathematical concepts in SSI using simpler expressions. In this method, the dynamic equilibrium equation of a structure was rewritten as a state-space equation. Next, the system matrices were obtained by numerical techniques such as QR decomposition, Singular Value Decomposition (SVD), or the least squares method. The modal parameters of the structure were determined using these matrices. In this method, the main parameter that affects the estimated modal parameters is the model order. The model order is actually the number of block rows in Hankel matrix. Rainieri and Fabbrocino [25] investigated the influence of model order on the accuracy of estimates via SSI. Reynders and De Roeck [26] suggested an equation to assign a low limit value to model order, which is a function of the sampling frequency, the lowest natural frequency of interest, and the number of measurement channels. Based on the use of their proposed equation and the results obtained from the initial tests, the lowest model order of 100 was obtained and used in modal identification. Brincker and Andersen [24] recommended conducting sensitivity analysis with respect to the model order to perform optimized modal parameter estimations. Therefore, sensitivity analysis for a range of 100 to 200 of model order values was conducted to identify the MDRs of the grid. The stabilization diagram of the output-only modal testing was plotted for the model order of 100 in Figure 5. A stabilization diagram is a graphical tool used to facilitate manual selection of the poles that are more likely to represent the physical modes of the structure. Stable, unstable, and noisy poles can be distinguished in accordance with the so-called stabilization criteria. The criteria for stable modes include maximum deviations of 0.0256 Hz from natural frequencies, 5% damping ratios, and 5%

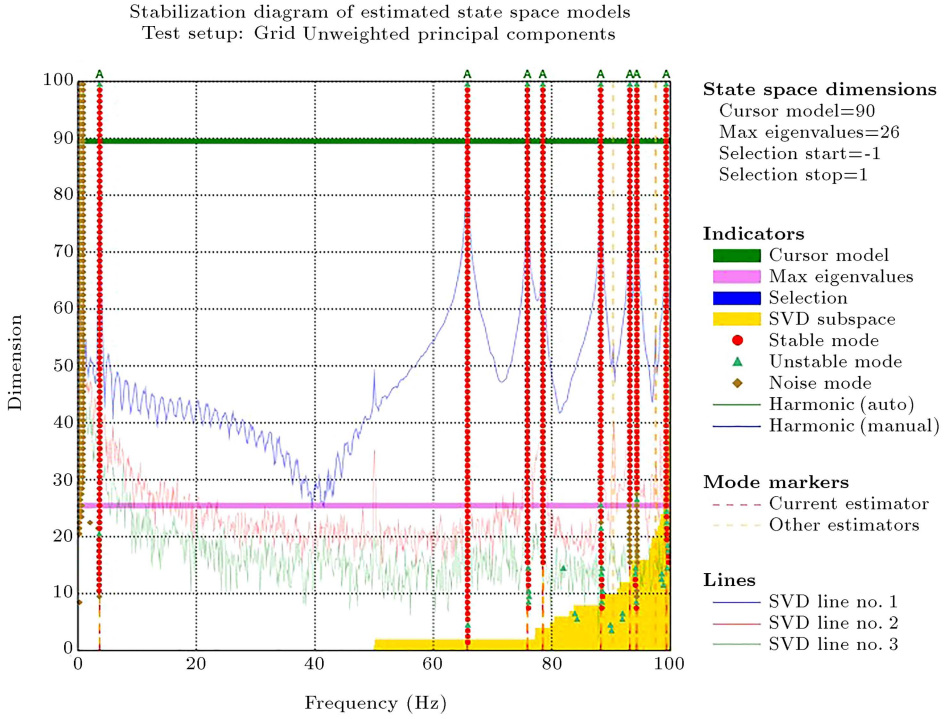

Figure 5. Stabilization diagram of modal testing for the model order of 100.

for MAC values between the modes which increase the system order;

EFDD: Compared to FDD, its enhanced version adds a modal estimation layer. The modal estimation is divided into two steps. The first step is to perform the FDD peak picking, while the second step is to use FDD identified mode shapes to identify the Single Degree Of Freedom (SDOF) spectral Bell functions. An SDOF correlation function is obtained by transferring the SDOF spectral Bell to the time domain. Then, through simple regression analysis, the estimates of both natural frequency as well as MDRs are obtained [27,28]. Tamura et al. [29] investigated the effect of frequency resolution on MDR estimates when the EFDD procedure is applied. It was shown that the estimated MDRs for all identified modes decreased when the frequency resolution improved. This result is true for all frequency-domain methods including CFDD. In this study, four different resolutions of 400, 800, 1600, and 3200 are considered in the frequency range of 0 to 100 Hz. Figure 6(a) shows the Average Normalized Power Spectral Density (ANPSD) of the measured responses for different resolutions. Figure 6(b) holds the same data as the previous one with a magnification range of 80–100 Hz. As revealed before, with an increase in the resolution, the peaks of the graph become sharper and thus, the MDR decreases;

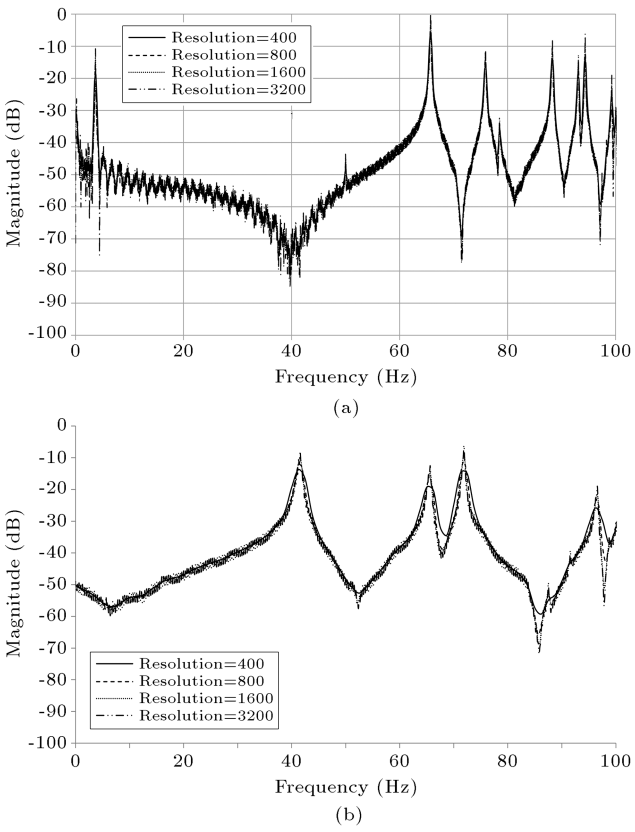

Figure 6. (a) Average Normalized Power Spectral Density (ANPSD) of responses for various frequency resolutions. (b) Magnification in the range of 80–10 Hz.

CFDD: The Curve-fit Frequency Domain Decomposition adds a modal estimation, similar to EFDD. The natural frequency and the MDRs of the mode are estimated by curve fitting the SDOF spectral Bell using frequency domain least-squares estimation. Since the SDOF spectral Bell is free from the influence of other modes, there is only a single eigenvalue and residue to fit. The natural frequency and the MDR are then extracted from eigenvalue [30].

5. Experimental results

The natural frequencies and the MDRs for the modes of interest were extracted using the methods mentioned in the previous section.

Upon using the SSI algorithm, the optimal choice of the model order affects the quality of modal parameter results. The natural frequencies and mode shapes are practically identified with sufficient accuracy; besides, the initial analysis corroborated that these parameters had not been affected upon significant changes in the model order as MDRs. Thus, this study directs its attention to sensitivity analysis of MDRs. Figures 7 to 11 show the results of sensitivity analysis of MDR estimates with respect to the model order, which were obtained through SSI-UPC algorithm. In these figures, Std. is the standard deviation of the identified MDRs for each model order, which represents the corresponding level of uncertainty. For the order of n, there are at most n values of identified MDRs, which Std. is the standard deviation of these values. As shown in these figures, the model order of 200 can be chosen as the optimal model order except for the MDR of the first mode. The MDR of the first mode identified via all SSI algorithms indicate a larger scatter than the other modes, which can be due to the limitation of

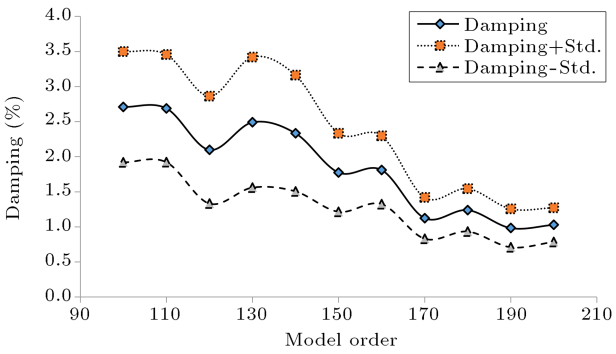

Figure 7. Variation of the Modal Damping Ratio (MDR) corresponding to the fist mode with respect to different model orders.

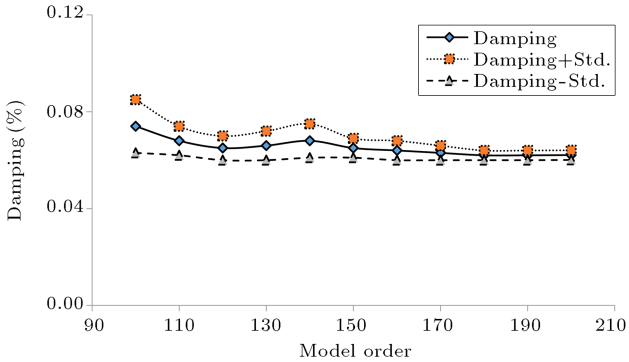

Figure 8. Variation of the Modal Damping Ratio (MDR) corresponding to the second mode with respect to different model orders.

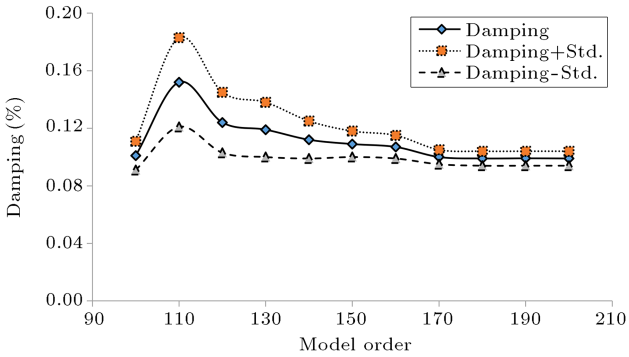

Figure 9. Variation of the Modal Damping Ratio (MDR) corresponding to the third mode with respect to different model orders.

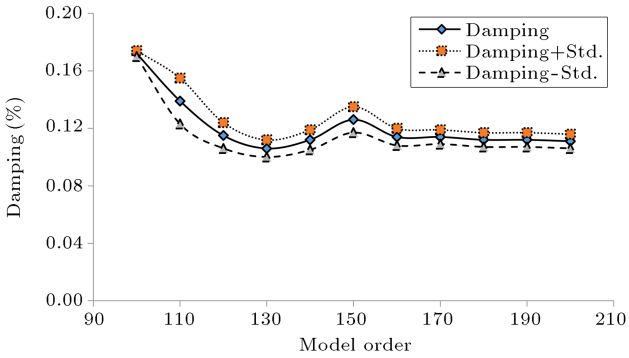

Figure 10. Variation of the Modal Damping Ratio (MDR) corresponding to the fourth mode with respect to different model orders.

accelerometers in the frequency range of the first mode of the grid.

In Tables 1 and 2, the results of the natural frequency and the MDR estimates for the grid obtained via SSI-UPC algorithm and different model order values of 100 to 200 are reported. As stated before, changes in the model order did not lead to significant changes in identified natural frequencies. According to Table 1, the natural frequencies of all modes except the

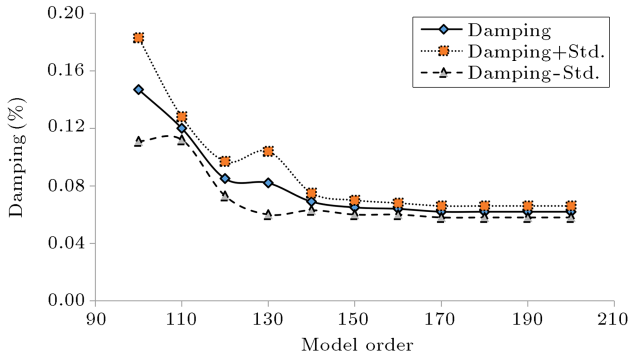

Figure 11. Variation of the Modal Damping Ratio (MDR) corresponding to the fifth mode with respect to different model orders .

seventh mode identified MDR of the first mode for all model orders. These results are true for the other two SSI algorithms. Although the MDRs of the first mode are subject to large dispersion in Table 2, convergence is obtained for the other modes.

Upon selecting the model order of 200 as the optimal order, the natural frequencies and MDRs were obtained via SSI algorithms for this model order and the results of the estimates together with their standard deviation values are given in Tables 3 and 4. In Table 3, the natural frequency estimates in each mode are very close to each other and the standard deviation is quite closer to zero, which indicates that the estimated results have a high level of certainty. According to Table 4, the MDR estimates in good agreement with each other are obtained from different SSI algorithms. Moreover, the largest difference of MDR values associated with the first mode, as already mentioned, is owing to the limitation of the accelerometers. Considerable scatter in the natural frequency and MDR estimates in the SSI-CVA algorithm result from the higher standard deviation values. As such, the SSI-PC algorithm is more efficient. However, the natural frequency as well as the MDR corresponding to the seventh mode of the grid were not identified using SSI algorithms.

In Tables 5 and 6, the natural frequency and MDR estimates identified through EFDD and CFDD are reported. In these tables, as previously stated, the resolution has been considered within a range of 400 to 3200. Very good agreement between the estimates of natural frequency obtained from the two methods can be observed in Table 5. In particular, the minimum difference of natural frequencies between the methods is observed at a resolution of 1600, indicating that this resolution is appropriate for the estimation of the natural frequency. In Table 6, the MDRs estimated through the EFDD and CFDD for all the identified modes, except the first mode, decrease when the frequency resolution improves. Moreover, on the contrary, the MDR estimates of the first mode were identified by the two methods and they had a significant difference,

Table 1. The natural frequency estimates of the grid identified via SSI-UPC.

Mode number	Order										
	100	**110**	**120**	**130**	**140**	**150**	**160**	**170**	**180**	**190**	**200**
1	3.64	3.63	3.65	3.67	3.66	3.66	3.65	3.67	3.67	3.67	3.67
2	65.74	65.75	65.74	65.74	65.74	65.74	65.74	65.74	65.74	65.74	65.74
3	75.88	75.87	75.90	75.90	75.90	75.89	75.90	75.89	75.90	75.90	75.90
4	78.48	78.49	78.48	78.48	78.48	78.48	78.47	78.48	78.48	78.48	78.48
5	88.24	88.29	88.28	88.27	88.28	88.28	88.28	88.28	88.28	88.28	88.28
6	93.17	93.14	93.11	93.11	93.09	93.08	93.08	93.09	93.06	93.08	93.08
7	94.33	94.34	94.35	94.34	94.33	—	—	—	94.36	—	—
8	99.33	99.31	99.31	99.34	99.32	99.29	99.26	99.25	99.29	99.28	99.28

Table 2. The Modal Damping Ratio (MDR) estimates of the grid identified via SSI-UPC.

Mode number	Order										
	100	**110**	**120**	**130**	**140**	**150**	**160**	**170**	**180**	**190**	**200**
1	2.71	2.69	2.10	2.49	2.33	1.78	1.81	1.13	1.24	0.98	1.03
2	0.07	0.07	0.07	0.07	0.07	0.07	0.06	0.06	0.06	0.06	0.06
3	0.10	0.15	0.12	0.12	0.11	0.11	0.11	0.10	0.10	0.10	0.10
4	0.17	0.14	0.12	0.11	0.11	0.13	0.11	0.11	0.11	0.11	0.11
5	0.15	0.12	0.09	0.08	0.07	0.07	0.06	0.06	0.06	0.06	0.06
6	0.17	0.08	0.09	0.10	0.11	0.09	0.09	0.08	0.09	0.09	0.08
7	0.08	0.07	0.06	0.06	0.05	—	—	—	0.06	—	—
8	0.19	0.19	0.16	0.18	0.18	0.15	0.15	0.12	0.10	0.11	0.10

Table 3. The natural frequency estimates of the grid together with their standard deviation identified via the Stochastic System Identification (SSI) algorithms.

Mode number	Method					
	UPC		**PC**		**CVA**	
	Freq. (Hz)	**Std. freq. (Hz)**	**Freq. (Hz)**	**Std. freq. (Hz)**	**Freq. (Hz)**	**Std. freq. (Hz)**
1	3.67	0.00	3.68	0.00	3.68	0.00
2	65.74	0.00	65.75	0.00	65.75	0.09
3	75.90	0.01	75.89	0.00	75.90	0.02
4	78.48	0.00	78.49	0.00	78.49	0.01
5	88.28	0.00	88.29	0.02	88.29	0.00
6	93.08	0.01	—	—	—	—
7	—	—	—	—	—	—
8	99.28	0.02	99.29	0.01	99.29	0.01

Table 4. The Modal Damping Ratio (MDR) estimates of the grid together with their standard deviation identified via Stochastic System Identification (SSI) algorithms.

Mode number	Method					
	UPC		**PC**		**CVA**	
	Damping (%)	**Std. damping (%)**	**Damping (%)**	**Std. damping (%)**	**Damping (%)**	**Std. damping (%)**
1	1.03	0.24	0.35	0.06	0.32	0.23
2	0.06	0.00	0.06	0.00	0.09	0.13
3	0.10	0.01	0.10	0.00	0.10	0.02
4	0.11	0.00	0.10	0.00	0.09	0.01
5	0.06	0.00	0.06	0.01	0.06	0.04
6	0.08	0.01	—	—	—	—
7	—	—	—	—	—	—
8	0.10	0.01	0.09	0.00	0.07	0.03

Table 5. The natural frequency estimates of the grid via Enhanced Frequency Domain Decomposition (EFDD) and Curve-fit Frequency Domain Decomposition (CFDD) (Hz).

Mode number	Frequency resolution							
	400		800		1600		3200	
	EFDD	CFDD	EFDD	CFDD	EFDD	CFDD	EFDD	CFDD
1	3.69	3.78	3.68	3.68	3.68	3.68	3.69	3.73
2	65.75	65.75	65.76	65.75	65.76	65.76	65.77	65.76
3	75.90	75.90	75.91	75.90	75.91	75.91	75.91	75.90
4	78.48	78.48	78.50	78.48	78.50	78.49	78.50	78.48
5	88.29	88.28	88.30	88.29	88.30	88.30	88.30	88.29
6	93.11	93.09	93.11	93.10	93.11	93.11	93.11	93.10
7	94.37	94.36	94.37	94.36	94.37	94.37	94.37	94.37
8	99.29	99.26	99.29	99.29	99.30	99.30	99.30	99.30

Table 6. The Modal Damping Ratio (MDR) estimates of the grid via Enhanced Frequency Domain Decomposition (EFDD) and Curve-fit Frequency Domain Decomposition (CFDD) (%).

Mode number	Frequency resolution							
	400		800		1600		3200	
	EFDD	CFDD	EFDD	CFDD	EFDD	CFDD	EFDD	CFDD
1	4.01	18.33	2.04	2.00	1.14	5.71	0.70	13.99
2	0.21	0.17	0.13	0.11	0.09	0.08	0.08	0.07
3	0.21	0.17	0.13	0.12	0.11	0.10	0.10	0.09
4	0.22	0.15	0.15	0.10	0.10	0.09	0.09	0.08
5	0.15	0.13	0.09	0.09	0.07	0.07	0.06	0.06
6	0.14	0.11	0.09	0.06	0.06	0.05	0.06	0.04
7	0.12	0.10	0.07	0.06	0.04	0.04	0.03	0.03
8	0.11	0.11	0.07	0.05	0.05	0.04	0.04	0.03

while there was good agreement for the MDR estimates of other modes. Likewise, the convergence of the MDR estimates of the second to eighth modes can be observed when the frequency resolution increases. However, there is no meaningful correlation for the MDR estimates of the first mode with the changes of resolution.

The difference between the MDR estimates of the second to eighth modes via EFDD and CFDD methods for different resolutions is illustrated in Figure 12. These differences decrease mainly when the resolution increases. The minimum difference between the MDR estimates by the two EFDD and CFDD methods was seen at a resolution of 1600, in which a similar conclusion was achieved for the natural frequency. Thus, this resolution was appropriate for identifying the grid and the corresponding results were selected to be compared with the results of the SSI algorithms.

6. Comparison and discussion

Based on a comparison of the results of natural frequency and MDR estimates obtained by the frequency domain methods (EFDD and CFDD) and time-domain methods (SSI algorithms), it can be concluded that time-domain methods managed to identify fewer modes than the frequency domain methods. Table 7 shows a comparison between the results provided by EFDD, CFDD, and three SSI algorithms. Since the first five modes of the grid were identified via all the methods, a comparison was made for these modes. Of note,

Table 7. Comparisons of the modal identification results.

Parameter	Mode number	SSI-UPC	SSI-PC	SSI-CVA	EFDD	CFDD
Natural frequency (Hz)	1	3.67	3.68	3.68	3.68	3.68
	2	65.74	65.75	65.75	65.76	65.76
	3	75.90	75.89	75.90	75.91	75.91
	4	78.48	78.49	78.49	78.50	78.49
	5	88.28	88.29	88.29	88.30	88.30
Damping ratio (%)	1	1.03	0.35	0.32	1.14	5.71
	2	0.06	0.06	0.09	0.09	0.08
	3	0.10	0.10	0.10	0.11	0.10
	4	0.11	0.10	0.09	0.10	0.09
	5	0.06	0.06	0.06	0.07	0.07

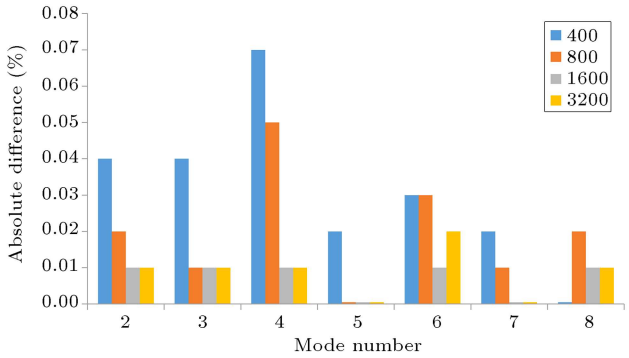

Figure 12. The difference of the Modal Damping Ratio (MDR) estimates obtained by Enhaced Frequency Domain Decomposition (EFDD) and Curve-fit Frequency Domain Decomposition (CFDD) methods.

Table 7 is constructed based on the model order of 200 for SSI algorithms as well as the resolution of 1600 for EFDD and CFDD methods. Very good agreement among the estimated natural frequencies identified via different methods can be observed, in which the highest difference corresponded to the first mode being equal to 0.27%. The difference in the MDR estimates was higher than in the natural frequencies due to the complicated nature. Regardless of the MDR estimate corresponding to the first mode, the results for third to fifth modes were in good agreement, but there was a difference rated at 50% for the MDR estimates of the second mode obtained from the methods.

7. Conclusions

In this paper, the Modal Damping Ratio (MDR) estimates of the first eight modes of a double-layer grid with the ball-joint system were experimentally determined. A physical model of the grid with necessity conditions was constructed. Free boundary conditions were considered for the grid. After applying an appropriate excitation to the grid, the acceleration responses of the grid were measured. The MDR estimates of the grid were obtained by output-only modal analysis.

A sensitivity analysis was performed to obtain the optimal model order for identification via the Stochastic System Identification (SSI) algorithms and the order of 200 was selected. Also, a frequency resolution of 1600 was chosen as an appropriate resolution for this grid upon using the frequency domain methods Enhanced Frequency Domain Decomposition (EFDD) and Curve-fit Frequency Domain Decomposition (CFDD) for identification of the modal parameters of the grid. The results of natural frequencies identified via five different methods showed good consistency in which the maximum relative difference between the methods was 0.27%. Regardless of the MDR estimates of the first mode, the MDRs identified by different methods were close to other modes. A large scatter in the estimates of the MDR was identified via output-only modal analysis to which some of the references referred were not observed in the present study. The maximum estimate of the MDR identified via different methods was 0.11% and such low damping of a double-layer grid with nonstructural components under free boundary conditions was reasonable.

References

1. Davoodi, M.R., Amiri, J.V., Gholampour, S., and Mostafavian, S.A. "Determination of nonlinear behavior of a ball joint system by model updating", *J. Constr. Steel Res.*, **71**, pp. 52–62 (2012).
2. Pashaei, M.H., Davoodi, M.R., and Nooshin, H. "Effects of tightness of bolts on the damping of a MERO-type double layer grid", *Int. J. Sp. Struct.*, **21**, pp. 103–110 (2006).

3. Naderpour, H., Barros, R.C., and Khatami, S.M. "A new model for calculating impact force and energy dissipation based on the CR-factor and impact velocity", *Scientia Iranica, A*, **22**(1), pp. 59–68 (2015).

4. Chopra, A.K. "Dynamics of structures: Theory and applications to earthquake engineering", *Prentice-hall International Series in Civil Engineering and Engineering Mechanics*, 4th Edn., Pearson, New Jersey, USA (2011).

5. Bajric, A., Georgakis, C.T., and Brincker, R. "Evaluation of damping using time domain OMA techniques", *Proc. SEM Fall Conf. Int. Symp. Intensive Load. Its Eff.*, Beijing, China., pp. 1–11 (2014).

6. Ren, W.-X., Peng, X.-L., and Lin, Y.-Q. "Experimental and analytical studies on dynamic characteristics of a large span cable-stayed bridge", *Eng. Struct.*, **27**, pp. 535–548 (2005).

7. Ren, W.-X., Zhao, T., and Harik, I.E. "Experimental and analytical modal analysis of steel arch bridge", *J. Struct. Eng.*, **130**(7), pp. 1022–1031 (2004).

8. Rainieri, C., Fabbrocino, G., and Cosenza, E. "Some remarks on experimental estimation of damping for seismic design of civil constructions", *Shock Vib.*, **17**, pp. 383–395 (2010).

9. Bajric, A., Brincker, R., and Thons, S. "Evaluation of damping estimates in the presence of closely spaced modes using operational modal analysis techniques", *6th International Operational Modal Analysis Conference*, Gijón, Spain (2015).

10. Gomaa, F., Tayel, M., Kandil, K., and Hekal, G. "Validation study illustrates the accuracy of operational modal analysis identification", *Int. J. Emerg. Technol. Adv. Eng.*, **2**, pp. 658–667 (2012).

11. Bajrić, A., Høgsberg, J., and Rüdinger, F. "Evaluation of damping estimates by automated operational modal analysis for offshore wind turbine tower vibrations", *Renew. Energy.*, **116**, pp. 153–163 (2018).

12. Kudu, F.N., Uçak, Ş., Osmancikli, G., Türker, T., and Bayraktar, A. "Estimation of damping ratios of steel structures by operational modal analysis method", *J. Constr. Steel Res.*, **112**, pp. 61–68 (2015).

13. Magalhães, F., Cunha, Á., Caetano, E., and Brincker, R. "Damping estimation using free decays and ambient vibration tests", *Mech. Syst. Signal Process.*, **24**, pp. 1274–1290 (2010).

14. Pridham, B.A. and Wilson, J.C. "A study of damping errors in correlation-driven stochastic realizations using short data sets", *Probabilistic Eng. Mech.*, **18**, pp. 61–77 (2003).

15. Chauhan, S. "Parameter estimation and signal processing techniques for operational modal analysis", PhD Thesis. University of Cincinnati, USA (2008).

16. Avitabile, P. "Modal space: Someone told me that operating modal analysis produces better results and that damping is much more realistic", *Exp. Tech.*, **30**, pp. 25–26 (2006).

17. Orlowitz, E. and Brandt, A. "Comparison of experimental and operational modal analysis on a laboratory test plate", *Measurement.*, **102**, pp. 121–130 (2017).

18. Mostafavian, S.A., Davoodi, M.R., and Vaseghi Amiri, J. "Ball joint behavior in a double layer grid by dynamic model updating", *J. Constr. Steel Res.*, **76**, pp. 28–38 (2012).

19. Brincker, R. and Ventura, C., *Introduction to Operational Modal Analysis*, 1st Ed., John Wiley & Sons, New Jersey, USA (2015).

20. ARTeMIS Modal 4, Issued by Structural Vibration Solutions AVS. NOVI Science Park, Niles Jernes Vej 10, DK 9220 Aalborg East, Denmark.

21. Van Overschee, P. and De Moor, B.L., *Subspace Identification for Linear Systems: Theory, Implementation, Applications*, 1st Edn., Springer Science & Business Media, Berlin, Germany (2012).

22. Rezvani, K., Maia, N.M.M., and Sabour, M.H. "A comparison of some methods for structural damage detection", *Scientia Iranica, B*, **25**(3), pp. 1312–1322 (2018).

23. Peeters, B. and De Roeck, G. "Stochastic system identification for operational modal analysis: A review", *J. Dyn. Syst. Meas. Control.*, **123**, p. 659 (2001).

24. Brincker, R. and Andersen, P. "Understanding stochastic subspace identification", *Proc. 24th IMAC, St. Louis*, Missouri, USA, pp. 279–311 (2006).

25. Rainieri, C. and Fabbrocino, G. "Influence of model order and number of block rows on accuracy and precision of modal parameter estimates in stochastic subspace identification", *Int. J. Lifecycle Perform. Eng.*, **1**, p. 317 (2014).

26. Reynders, E. and De Roeck, G. "Reference-based combined deterministic-stochastic subspace identification for experimental and operational modal analysis", *Mech. Syst. Signal Process.*, **22**, pp. 617–637 (2008).

27. Brincker, R., Ventura, C.E., and Andersen, P. "Damping estimation by frequency domain decomposition", *19th International Modal Analysis Conference*, Orlando, Fl, USA, pp. 698–703 (2001).

28. Wang, T., Celik, O., Catbas, F.N., and Zhang, L.M. "A frequency and spatial domain decomposition method for operational strain modal analysis and its application", *Engineering Structures*, **114**, pp. 104–112 (2016).

29. Tamura, Y., Yoshida, A., Zhang, L., Ito, T., Nakata, S., and Sato, K. "Examples of modal identification of structures in Japan by FDD and MRD techniques",

Proc. 1st Int. Oper. Modal Anal. Conf. IOMAC, Copenhagen, Denmark (2005).

30. Jacobsen, N.J., Andersen, P., and Brincker, R. "Applications of frequency domain curve-fitting in the EFDD technique", In *Proceedings IMAC XXVI Conference*, Orlando, FL, USA (2008).

Biographies

Seyed Rasoul Nabavian received PhD degree in Structural Engineering from Babol Noshirvani University of Technology, Babol, Iran in 2019. His current research interests include operational modal analysis and noise modeling.

Mohammad Reza Davoodi received PhD degree in Civil Engineering from University of Surrey, Guildford, England in 2004. He was an Associate Professor at Babol Noshirvani University of Technology, Babol, Iran. He passed away with Covid-19 on 7 April, 2020. Peace be upon him.

Bahram Navayi Neya received PhD degree in Civil Engineering from University of Tarbiate Modarres, Tehran, Iran in 2002. Now, he is a Professor of Structural Engineering at Babol Noshirvani University of Technology, Babol, Iran. His current research interests include damage detection and modal analysis.

Seyedamin Mostafavian received PhD degree in Civil Engineering from Babol Noshirvani University of Technology, Babol, Iran in 2012. Now, he is an Assistant Professor at Payame Noor University (PNU), Tehran, Iran. His current research interests include operational modal analysis.